SPECTRAL ANALYSIS OF SEISMIC WAVES : PART 1. DATA WINDOWS FOR THE ANALYSIS OF TRANSIENT WAVES

AUTHOR(S):

KURITA, Tuneto

CITATION:

KURITA, Tuneto. SPECTRAL ANALYSIS OF SEISMIC WAVES : PART 1. DATA WINDOWS FOR THE ANALYSIS OF TRANSIENT WAVES. Special Contributions of the Geophysical Institute, Kyoto University 1969, 9: 97-122

ISSUE DATE:

1969-12

URL:

http://hdl.handle.net/2433/178567

Special Contributions, Geophysical Institute, Kyoto University, No. 9, 1969, 97-122

SPECTRAL ANALYSIS OF SEISMIC WAVES
PART 1. DATA WINDOWS FOR THE ANALYSIS OF TRANSIENT WAVES

By

Tuneto KURITA*

(Received October 11, 1969)

Abstract

Causes of strong undulations generally observed in the spectra of seismic initial phases have been theoretically investigated and attributed to the effects of the sharp truncation of signals and of the incidence of later phases. Characteristics of observed amplitude and phase spectra have been shown to coincide well with theoretical considerations. In order to derive the fine structure of the spectra of initial phases, the choice of data windows suitable for the purpose and the selection of an appropriate time interval of analysis to exclude the effects of later phases are indispensable. Further, in the spectral analysis of seismograms, care must be taken over the worsening of spectra caused by the simplification of analytical procedure, namely, the reversion of the order of steps, correction of instrumental response and superposition of data windows, especially when a "heavy" data window is applied. The behavior of data windows to be superposed on initial phases and that of the corresponding spectral windows have been examined in detail.

1. Introduction

Spectral analysis of body waves, especially of *P*-waves, is now one of the most powerful sources of information in many branches of seismological study.

It is known from observations that the effects of the truncation of signal tail and of the incidence of later phases on the amplitude and phase spectra of the initial phase are significant. These effects will be theoretically examined and compared with observational results.

In the spectral analysis of transient waves, it is inevitable to superpose a data window on the signal, for otherwise a rectangular data window will necessarily be superposed, which behaves badly in the frequency domain. The behavior of spectral windows corresponding to some typical data windows and their effects on the spectra of signals will be examined in some detail, and what

* Department of Transportation Engineering, Faculty of Engineering, Kyoto University.

kind of data windows should be used will be pursued. Generally in the analysis of seismograms, two steps of the spectral procedure, (i) correction of instrumental response and (ii) superposition of a data window, are applied in reverse order for analytical convenience. The difference in the spectra resulting from the reverse order and appropriate procedures will be examined with some examples.

2. Data windows and the corresponding spectral windows

Almost all discussions on the window for the spectral analysis of waves seem to have rested on the methodology in the filtering of waves to extract waves of a particular frequency range.

Let $f(t)$ be a time series, $w(t)$ a weight function and $\bar{f}(t)$ the convolution of $f(t)$ with $w(t)$, and $F(\omega)$, $W(\omega)$ and $\bar{F}(\omega)$, the Fourier transforms of these functions, then we obtain the next relation between them.

$$\begin{array}{ccc} f(t) & w(t) & \xrightarrow{\text{convolution}} f(t)*w(t) \equiv \bar{f}(t) \\ \updownarrow & \updownarrow & \\ F(\omega) & W(\omega) & \xrightarrow{\text{multiplication}} F(\omega)W(\omega) \equiv \bar{F}(\omega) \end{array} \qquad (1)$$

In the above, an asterisk indicates the convolution and arrows with two apices show that the two functions are related to each other as Fourier pairs. Therefore, if we wish to take out waves of a limited frequency range, we convolve a given time series, $f(t)$, with a weight function, $w(t)$. The weight function should be determined from the Fourier transformation of its frequency response, $W(\omega)$. Methods of low-pass, high-pass and band-pass filterings are given, for example, in Holloway [1958], Papoulis [1962] or Wood [1968]. All data windows in Table 1 act as low-pass filters when they are convolved with a time series.

In the spectral analysis of body waves, however, we generally intend to obtain the undistorted spectra, but not to take out waves of a particular frequency range. Their transient aspects introduce some unfavourable effects into the spectral analysis of seismograms. The frequency resolution of spectra are limited by the finiteness of the length of analysis. The resolution in cps is generally equal to the reciprocal of the total length of analysis in seconds. Further, to take a finite length of analysis on the record is equivalent to passing the record through a rectangular window, which distorts the spectra of a signal as seen below. This is pointed out, for example, in Fernandez and Careage [1968]. Therefore, a data window with the exception of the rectangular window should be superposed on the signal.

From relation (1) and symmetry property of the Fourier pair, it follows that

$$\begin{array}{cc} f(t) & w(t) \\ \updownarrow & \updownarrow \\ F(\omega) & W(\omega) \end{array} \xrightarrow{\text{multiplication}} \begin{array}{cc} f(t) & w(t) \\ & \updownarrow \\ & \bar{F}(\omega) \end{array} \equiv \bar{f}(t)$$
$$\xrightarrow{\text{convolution}} \frac{1}{2\pi} F(\omega) * W(\omega) \equiv \bar{F}(\omega) \qquad (2)$$

From this relation, it appears that when a data window is superposed on the record to exclude the truncation effect, averaging of spectra at given frequencies by the neighbouring spectra will occur. This is unavoidable for the spectral analysis of records with a limited length.

We will examine in some detail how the amplitude and phase spectra of a signal, $f(t)$ are affected by the superposition of a data window, $w(t)$. When the Fourier pair, $f(t)$ and $F(\omega)$, and the cosine and sine transforms of $f(t)$, $a(\omega)$ and $b(\omega)$, are represented by

$$f(t) = \frac{1}{2\pi}\int_{-\infty}^{\infty} F(\omega)\exp(i\omega t)d\omega,$$

$$F(\omega) = \int_{-\infty}^{\infty} f(t)\exp(-i\omega t)dt = A(\omega)\exp(iP(\omega)),$$

and

$$a(\omega) = \int_{-\infty}^{\infty} f(t)\cos\omega t dt,$$

$$b(\omega) = \int_{-\infty}^{\infty} f(t)\sin\omega t dt,$$

then

$$F(\omega) = a(\omega) - ib(\omega).$$

From this expression and relation (2), we have

$$\left.\begin{aligned} \bar{F}(\omega) &= \frac{1}{2\pi}\int_{-\infty}^{\infty} F(\omega-\omega')W(\omega')d\omega' \\ &= \frac{1}{2\pi}\int_{-\infty}^{\infty} a(\omega-\omega')W(\omega')d\omega' - \frac{1}{2\pi}\int_{-\infty}^{\infty} b(\omega-\omega')W(\omega')d\omega'. \end{aligned}\right\} \qquad (3)$$

Thus, denoting the amplitude and phase spectra of $\bar{F}(\omega)$ by $\bar{A}(\omega)$ and $\bar{P}(\omega)$, we have

$$\left.\begin{aligned} \bar{A}(\omega) &= (\bar{a}(\omega)^2 + \bar{b}(\omega)^2)^{1/2}, \\ \bar{P}(\omega) &= \tan^{-1}(-\bar{b}(\omega)/\bar{a}(\omega)), \end{aligned}\right\} \qquad (4)$$

where $\bar{a}(\omega)$ and $-\bar{b}(\omega)$ are the real and imaginary parts of $\bar{F}(\omega)$.

When $w(t)$ is an even function, $W(\omega)$ is real, and then $\bar{a}(\omega)$ and $\bar{b}(\omega)$ are represented by

$$\left.\begin{aligned} \bar{a}(\omega) &= \frac{1}{2\pi}\int_{-\infty}^{\infty} a(\omega-\omega')W(\omega')d\omega', \\ \bar{b}(\omega) &= \frac{1}{2\pi}\int_{-\infty}^{\infty} b(\omega-\omega')W(\omega')d\omega'. \end{aligned}\right\} \qquad (5)$$

Thus, it appears that when the data window is superposed on the signal, both the cosine and sine transforms at given frequencies are averaged over their neighbouring ones with the weight, the spectral window corresponding to

the data window.

Now we adopt the rectangular window for $W(\omega)$. We introduce a function $p_T(t)=1$ for $|t|\leq T$ and 0 for $|t|>T$, its Fourier transform being $2\sin\omega T/\omega$. Denoting the Fourier pairs by $f(t)\leftrightarrow F(\omega)$ and $f(t)p_T(t)\leftrightarrow F_T(\omega)$, we obtain from relation (2)

$$\left.\begin{aligned} F_T(\omega)&=\frac{1}{2\pi}F(\omega)*\frac{2\sin\omega T}{\omega}\\ &=\int_{-\infty}^{\infty}F(\omega-\omega')\frac{\sin\omega' T}{\pi\omega'}d\omega'. \end{aligned}\right\} \tag{6}$$

This means that the Fourier transform of a truncated record is an average of the signal spectrum, $F(\omega)$ by the Fourier transform of the rectangular window, $p_T(t)$.

In expression (6), the second term in the integrand tends to the impulse response $\delta(\omega)$ as T tends to infinity,

$$\lim_{T\to\infty}\frac{\sin\omega' T}{\pi\omega'}=\delta(\omega').$$

Therefore, it follows that

$$\lim_{T\to\infty}F_T(\omega)=\int_{-\infty}^{\infty}F(\omega-\omega')\delta(\omega')d\omega.$$

Since the last integral is equal to $F(\omega)$ for every continuity point, it follows that if the time interval of analysis is sufficiently long, $F_T(\omega)$ reduces to $F(\omega)$.

Table 1. Data windows and corresponding spectral windows.

Data window		Spectral window
Rectangular window		
$w_1(t)=\frac{1}{T}$	$\lvert t\rvert\leq T$	$W_1(\omega)=\frac{2\sin\omega T}{\omega T}$
$=0$	$\lvert t\rvert>T$	
Power window		
$w_2(t)=\frac{1}{T}\left\{1-\left(\frac{\lvert t\rvert}{T}\right)^n\right\}$	$\lvert t\rvert\leq T$	$W_2(\omega)=\frac{2\sin\omega T}{\omega T}-\frac{2}{T^{n+1}}K(\omega)$
$=0$	$\lvert t\rvert>T$	n; even
(n; positive integer)		$K(\omega)=\sin\omega T\sum_{k=0}^{n/2}(-1)^k\frac{T^{n-2k}}{\omega^{2k+1}}\frac{n!}{(n-2k)!}$
		$+\cos\omega T\sum_{k=1}^{n/2}(-1)^{k-1}\frac{T^{n-2k+1}}{\omega^{2k}}\frac{n!}{(n-2k+1)!}$
		n; odd
		$K(\omega)=\sin\omega T\sum_{k=0}^{(n-1)/2}(-1)^k\frac{T^{n-2k}}{\omega^{2k+1}}\frac{n!}{(n-2k)!}$
		$+\cos\omega T\sum_{k=1}^{(n+1)/2}(-1)^{k-1}\frac{T^{n-2k+1}}{\omega^{2k}}\frac{n!}{(n-2k+1)!}$
		$+(-1)^{(n+1)/2}\frac{n!}{\omega^{n+1}}$

Triangular window $w_3(t)=\frac{1}{T}\left\{1-\frac{\lvert t\rvert}{T}\right\}$ $=0$	$\lvert t\rvert\leq T$ $\lvert t\rvert>T$	$W_3(\omega)=\left\{\frac{\sin(\omega T/2)}{\omega T/2}\right\}^2$
Fourier kernel window $w_4(t)=\frac{1}{T}\frac{\sin(\pi t/T)}{\pi t/T}$ $=0$	$\lvert t\rvert\leq T$ $\lvert t\rvert>T$	Fig. 2
$w_4'(t)=\frac{1}{T}\frac{\sin(\pi t/T)}{\pi t/T}$		$W_4'(\omega)=1$ $\lvert\omega\rvert\leq\frac{\pi}{T}$ $=0$ $\lvert\omega\rvert>\frac{\pi}{T}$
Fejér kernel window $w_5(t)=\frac{1}{T}\left\{\frac{\sin(\pi t/T)}{\pi t/T}\right\}^2$ $=0$	$\lvert t\rvert\leq T$ $\lvert t\rvert>T$	Fig. 2
$w_5'(t)=\frac{1}{T}\left\{\frac{\sin(\pi t/T)}{\pi t/T}\right\}^2$		$W_5'(\omega)=1-\frac{\lvert\omega\rvert T}{2\pi}$ $\lvert\omega\rvert\leq\frac{2\pi}{T}$ $=0$ $\lvert\omega\rvert>\frac{2\pi}{T}$
Hanning window $w_6(t)=\frac{1}{2T}\left\{1+\cos\frac{\pi t}{T}\right\}$ $=0$	$\lvert t\rvert\leq T$ $\lvert t\rvert>T$	$W_6(\omega)=\frac{\sin\omega T}{\omega T}$ $+0.5\left\{\frac{\sin(\omega+\pi/T)T}{(\omega+\pi/T)T}+\frac{\sin(\omega-\pi/T)T}{(\omega-\pi/T)T}\right\}$ $=\frac{(\pi/T)^2}{(\pi/T)^2-\omega^2}\frac{\sin\omega T}{\omega T}$
Hamming window $w_7(t)=\frac{1}{T}\left\{0.54+0.46\cos\frac{\pi t}{T}\right\}$ $=0$	$\lvert t\rvert\leq T$ $\lvert t\rvert>T$	$W_7(\omega)=1.08\frac{\sin\omega T}{\omega T}$ $+0.46\left\{\frac{\sin(\omega+\pi/T)T}{(\omega+\pi/T)T}+\frac{\sin(\omega-\pi/T)T}{(\omega-\pi/T)T}\right\}$
Gaussian window $w_8(t)=\frac{1}{T}\exp\left(-\frac{t^2}{2\sigma^2}\right)$ $=0$	$\lvert t\rvert\leq T$ $\lvert t\rvert>T$	$W_8(\omega)=\frac{2\sqrt{2}\sigma}{T}\exp\left(-\frac{\sigma^2\omega^2}{2}\right)\mathrm{Erf}\left(\frac{T}{\sqrt{2}}\right)^*$
$w_8'(t)=\frac{1}{T}\exp\left(-\frac{t^2}{2\sigma^2}\right)$		$W_8'(\omega)=\frac{\sqrt{2\pi}\sigma}{T}\exp\left(-\frac{\sigma^2\omega^2}{2}\right)$

* Erf represents the error function $\mathrm{Erf}(x)=\int_0^x\exp(-t^2)dt$

However, the spectrum resulting from the signal truncated by a short interval is only an average which is a poor estimation of spectra of signal.

To remedy this difficulty, Kurita [1966] utilized $w_2(t)$ in Table 1. This data window is useful in two respects that its use equalizes the amplitude of

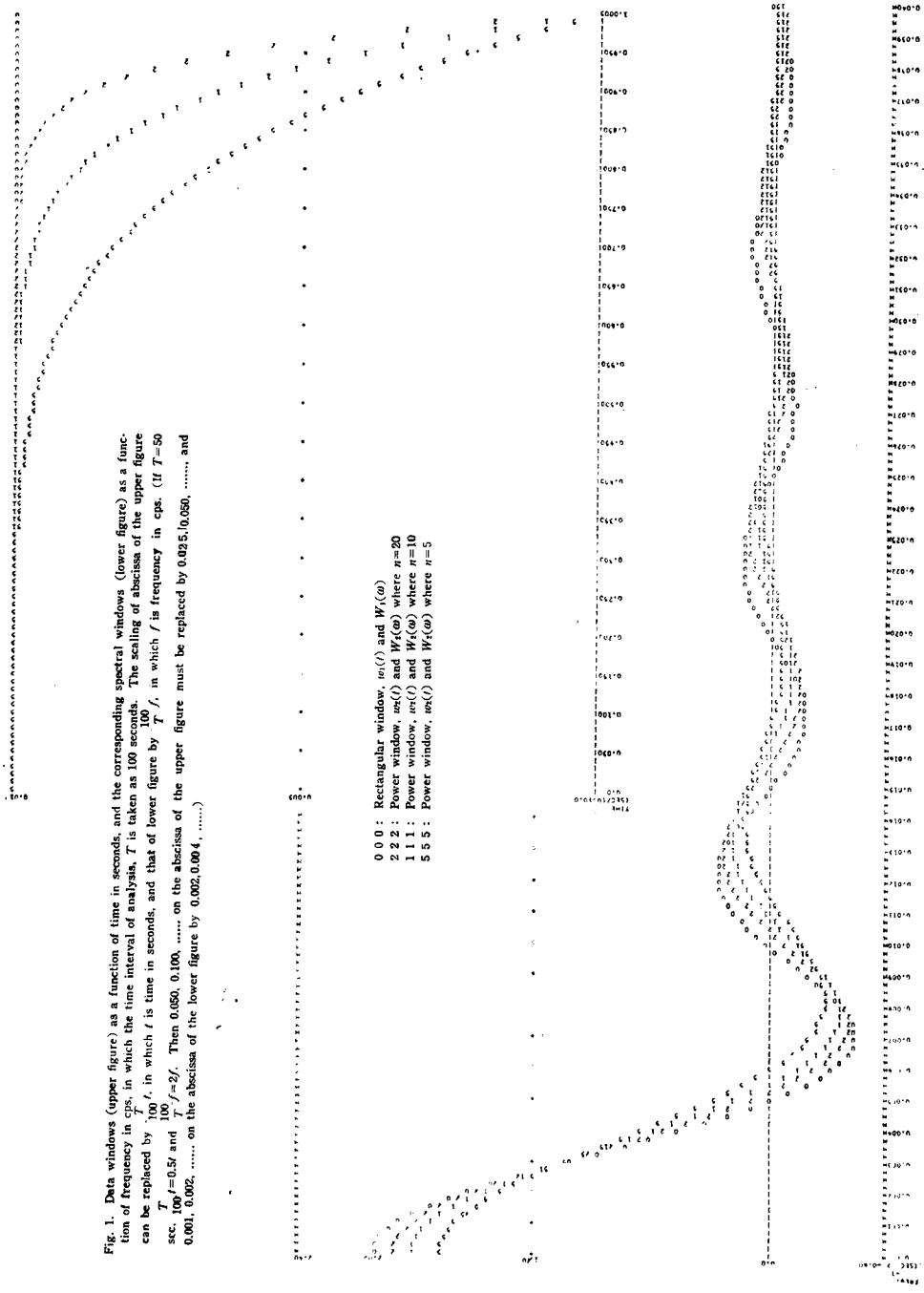

Fig. 1. Data windows (upper figure) as a function of time in seconds, and the corresponding spectral windows (lower figure) as a function of frequency in cps, in which the time interval of analysis, T is taken as 100 seconds. The scaling of abscissa of the upper figure can be replaced by $\frac{T}{100}t$, in which t is time in seconds, and that of lower figure by $\frac{100}{T}f$, in which f is frequency in cps. (If $T=50$ sec, $\frac{T}{100}f=0.5f$ and $\frac{100}{T}f=2f$. Then 0.050, 0.100, ... on the abscissa of the upper figure must be replaced by 0.025, 0.050, ..., and 0.001, 0.002, ... on the abscissa of the lower figure by 0.002, 0.004, ...)

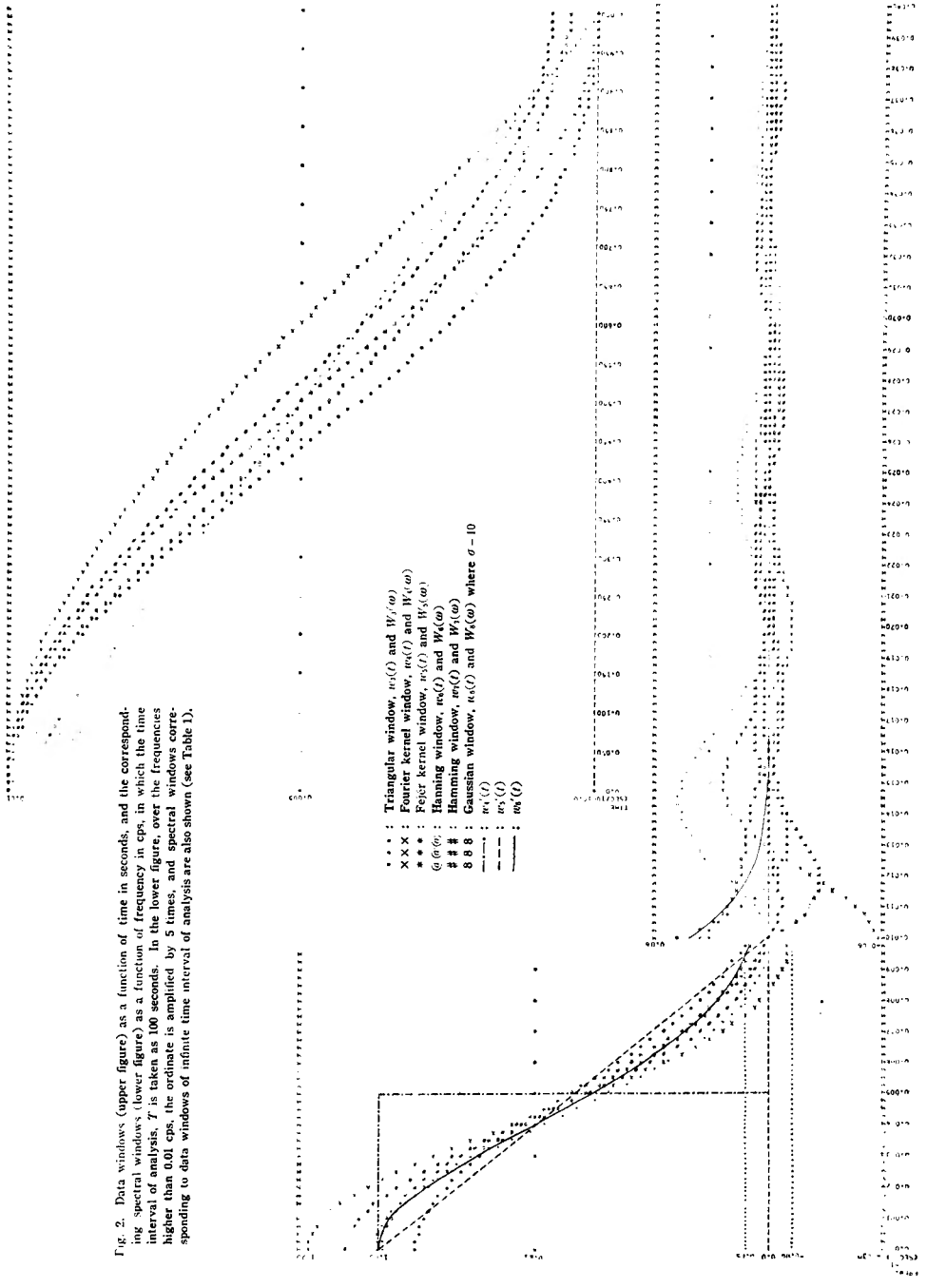

Fig. 2. Data windows (upper figure) as a function of time in seconds, and the corresponding spectral windows (lower figure) as a function of frequency in cps, in which the time interval of analysis, T is taken as 100 seconds. In the lower figure, over the frequencies higher than 0.01 cps, the ordinate is amplified by 5 times, and spectral windows corresponding to data windows of infinite time interval of analysis are also shown (see Table 1).

a signal at the truncation point to that at the beginning point, and that the amplitude of undulation of the corresponding spectral window, $W_2(\omega)$ is small compared with $W_1(\omega)$ corresponding to $w_1(t)$. The smaller n becomes, the less the amplitude of undulation of $W_2(\omega)$ is, as is apparent in Fig. 1. The value of n should be determined by the behavior of signal near the truncation point. This data window is appropriate for the spectral analysis of waves with rather short time length, less than about 50 to 60 seconds, and particularly for an isolated signal, which brings useful information into seismology.

Other typical data windows and their corresponding spectral windows are tabulated in Table 1 and shown in Fig. 2. Since a complete data window does not exist, we must select a window most suitable to the purpose of analysis.

We notice once again that when a data window $w(t)$ is superposed on a signal, its amplitude and phase spectra are averaged by $W(\omega)$ as in expressions (3), or (4) and (5). Therefore, we should select a well-behaved window with small sidelobes as far as possible. In the spectral analysis of transient P-waves, in addition to averaging effects in the frequency domain, data windows except $w_1(t)$ act as weighting functions which emphasize the initial part of signal and lessen the effects of later phases.

$w_1(t)$ and $w_4(t)$ are symmetrical with each other. As $W_4(\omega)$ is ill-behaved as is apparent in Fig. 2, $w_4(t)$ is tabulated only for comparison.

$w_3(t)$ and $w_5(t)$ are also symmetrical with each other. $w_3(t)$ can be regarded as a special case of $w_2(t)$ when $n=1$. $w_5(t)$ is the most "heavy" window in Table 1 in the sense that it strongly supresses the later part of a time interval of analysis. The corresponding spectral window $W_5(\omega)$ is well-behaved. Therefore, it has been utilized by Kurita [1969] for the body wave method of determining the crustal and upper mantle structure, in which the time interval of analysis is generally about 100 seconds or more. To estimate the phase spectrum of a signal, it is desirable that $W(\omega)$ be "heavy", for otherwise the phase spectrum varies severely with frequency, as is easily surmised from expression (4).

$w_6(t)$ and $w_7(t)$ are familiar Hanning and Hamming windows. The spectral window corresponding to Hamming window is rather better-behaved than Hanning window, but Hamming window is not zere and 8 parts in 100 at the end of an analyzed interval.

$w_8(t)$, Gaussian window also is not zero at the end of an analyzed interval, though its behavior in the spectral domain is rather well. In Fig. 2 σ is taken as 40.

In order to obtain spectra of transients, superposing a data window on the record of the signal is generally preferred to averaging the spectra of signal

by the corresponding spectral window, because the procedure is simpler for the data window and its use excludes the effect due to the inequality of the signal amplitude at the end of the time interval of analysis and that at the beginning of it.

3. Data windows and correction of instrumental response

Generally in the spectral analysis of seismograms, for simplicity, we first superpose a data window on the record, make a Fourier analysis and then correct the resultant spectra by the instrumental response, although strictly speaking this is incorrect. With $f_s(t)$ and $F_s(\omega)$, the instrumental response and the corresponding Fourier transform, this procedure corresponds to steps (A) and (B) in the next relation.

$$\begin{array}{ccc} f(t)\quad w(t)\equiv f_1(t) & \longrightarrow & f_1(t)*\dfrac{1}{f_s(t)}\equiv \bar{f}(t) \\ \downarrow \qquad (\mathrm{A})\downarrow\uparrow & & \downarrow \\ \dfrac{1}{2\pi}F(\omega)*W(\omega)\equiv F_1(\omega) & \xrightarrow{(\mathrm{B})} & F_1(\omega)/F_s(\omega)\equiv \bar{F}(\omega). \end{array} \tag{7}$$

The due analytical procedure, however, must be that we first correct the record by the instrumental response, superpose a data window and then Fourier analyze it. There are many ways shown by arrows in the next relation, in order to obtain $\bar{F}(\omega)$.

$$\begin{array}{ccc} f(t)*\dfrac{1}{f_s(t)}\equiv f_2(t) & \xrightarrow{(\mathrm{C})} & f_2(t)\quad w(t)\equiv \bar{f}(t) \\ \downarrow(\mathrm{A}) \qquad \downarrow\uparrow(\mathrm{B}) & & \downarrow(\mathrm{D}) \\ F(\omega)/F_s(\omega)\equiv F_2(\omega) & \xrightarrow{(\mathrm{E})} & \dfrac{1}{2\pi}F_2(\omega)*W(\omega)\equiv \bar{F}(\omega). \end{array} \tag{8}$$

It is difficult as a numerical procedure to take the inversion of $f_s(t)$ and convolve it with $f(t)$. Then the first step must be (A). The second step may prefer (B) to (E), for in the step (E) the spectral window $W(\omega)$ should differ

Table 2. Information on the records used for the present study.

Record No. 1	Z-, EW- and NS-components of long-period seismograph system (USCGS, T_0=15 sec, T_g=100 sec, h_0=1.0, h_g=1.0, σ=0, Mag=6000) recorded at Matsushiro (MAT) for a shallow shock occurred at Nepal-India border region on June 27, 1966 (Shock No. 12 of Table 2 in the article of Kurita [1969]). Epicentral distance and azimuth from MAT are 47.9° and 279.2°, respectively.
Record No. 2	Z- and EW-components of long-period seismograph system recorded at MAT for an intermediate shock occured at Afghanistan-USSR border region on June 6, 1966 (Shock No. 14 of Table 2 in the article of Kurita [1969]). Epicentral distance and azimuth from MAT are 52.9° and 291.1°, respectively.

Fig. 3(a). Comparisons of amplitude (upper figure) and phase (lower figure) spectra of vertical and horizontal components of P-waves as a function of frequency in cps, for different data windows and analytical procedures, for the record No. 1 in Table 2. The analyzed waveforms of Z ( ), EW- (– – –) and NS- (····) components as a function of time in seconds are shown in the right half of the upper figure. The time interval of analysis is about 114 seconds.

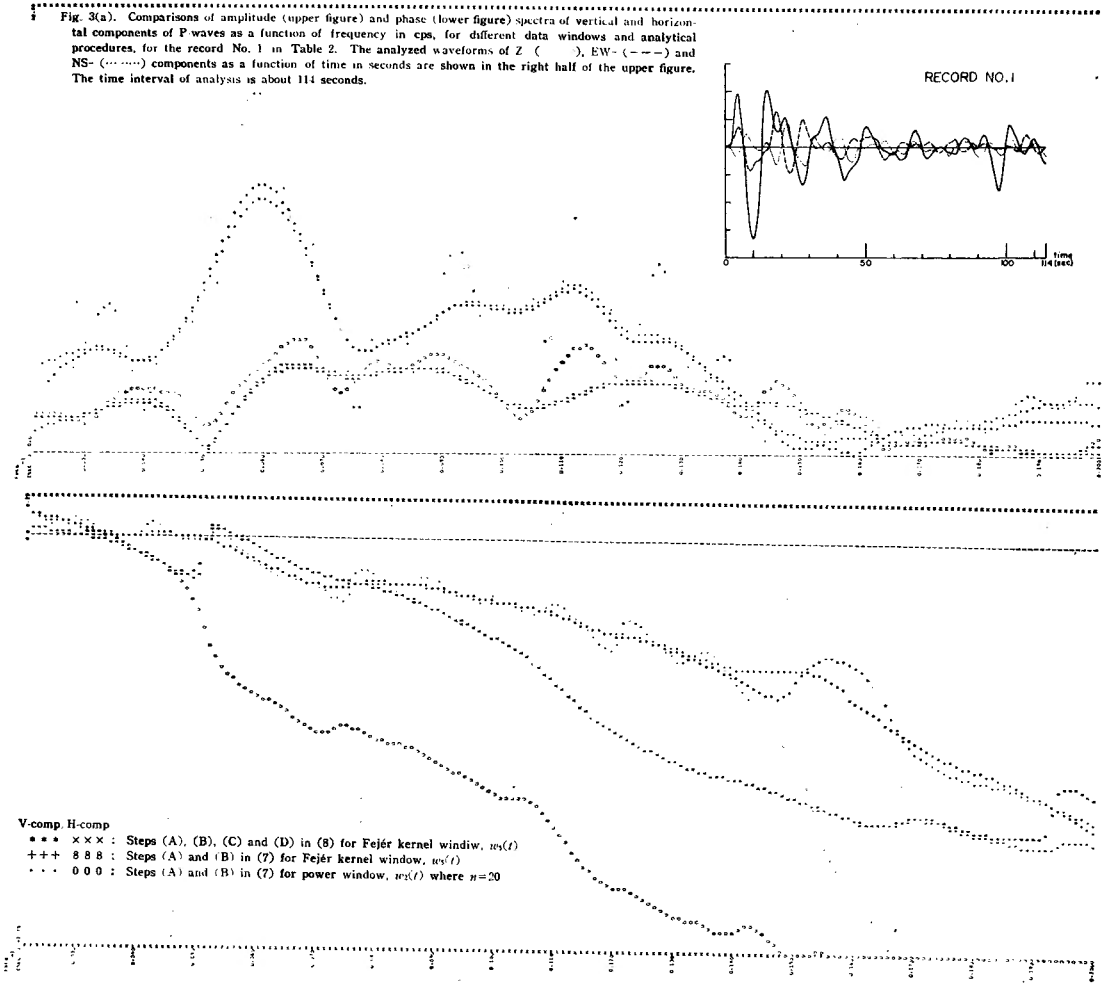

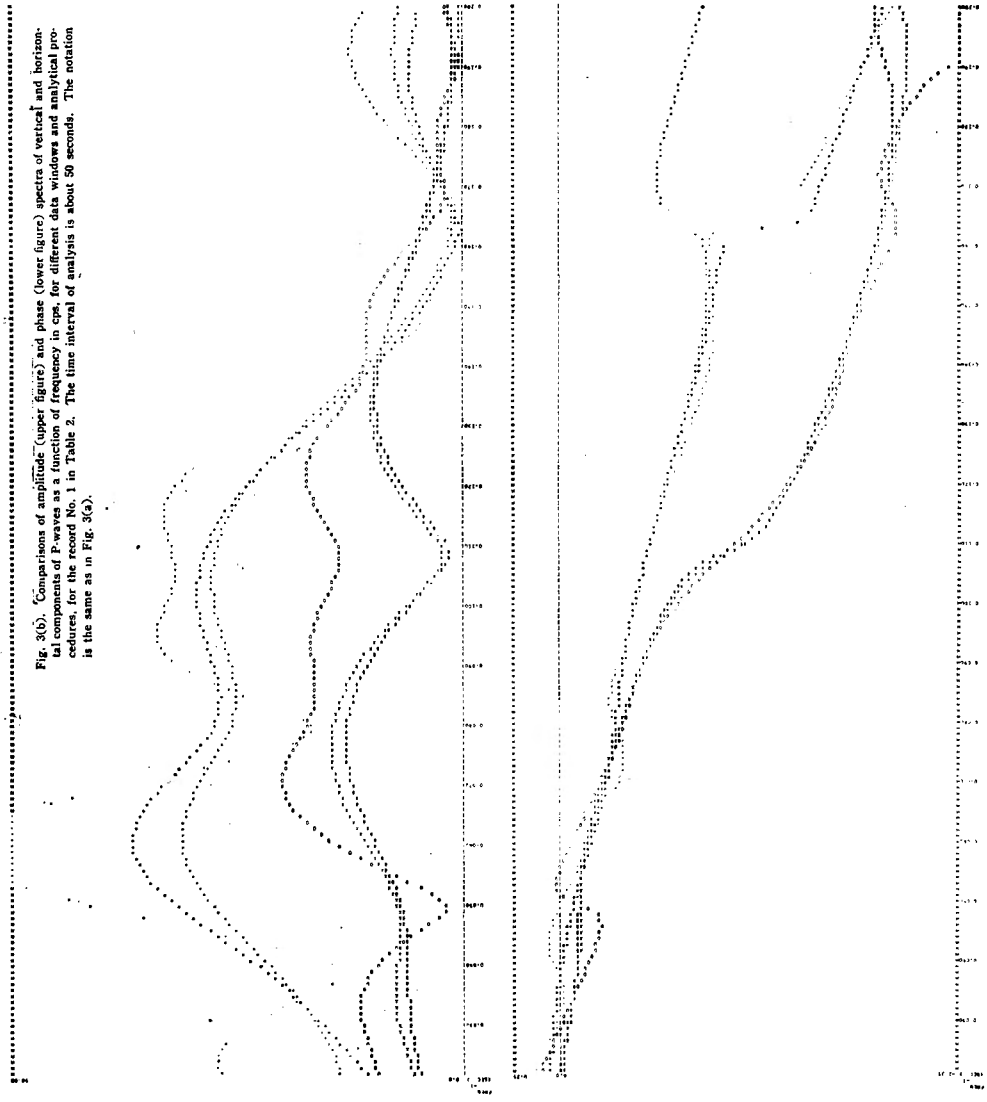

Fig. 3(b). Comparisons of amplitude (upper figure) and phase (lower figure) spectra of vertical and horizontal components of P-waves as a function of frequency in cps, for different data windows and analytical procedures, for the record No. 1 in Table 2. The time interval of analysis is about 50 seconds. The notation is the same as in Fig. 3(a).

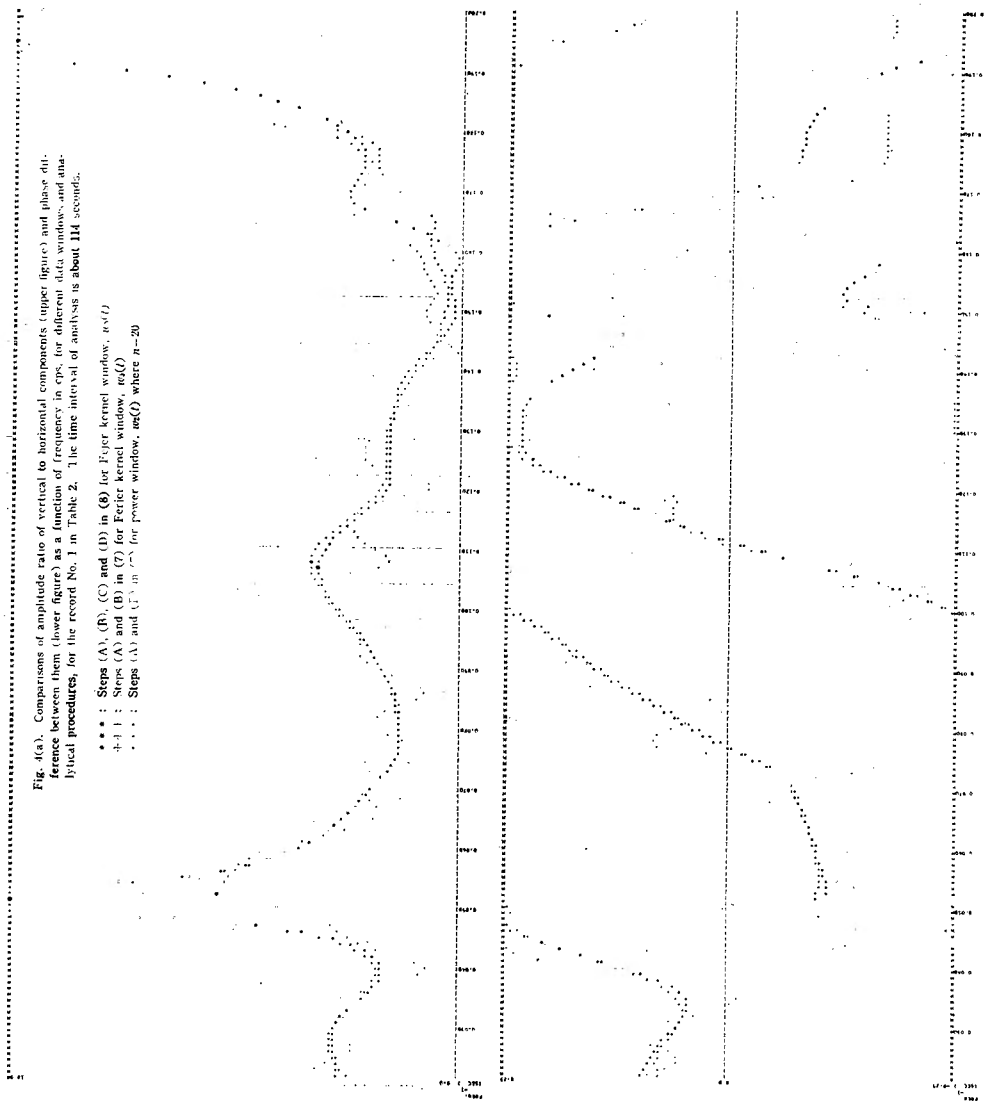

Fig. 4(a). Comparisons of amplitude ratio of vertical to horizontal components (upper figure) and phase difference between them (lower figure) as a function of frequency in cps, for different data windows and analytical procedures, for the record No. 1 in Table 2. The time interval of analysis is about 114 seconds.

* * * : Steps (A), (B), (C) and (D) in (8) for Fejer kernel window, $w_1(j)$
+ + + : Steps (A) and (B) in (7) for Fejer kernel window, $w_2(j)$
. . . : Steps (A) and (C) in (7) for power window, $w_3(j)$ where $n=20$

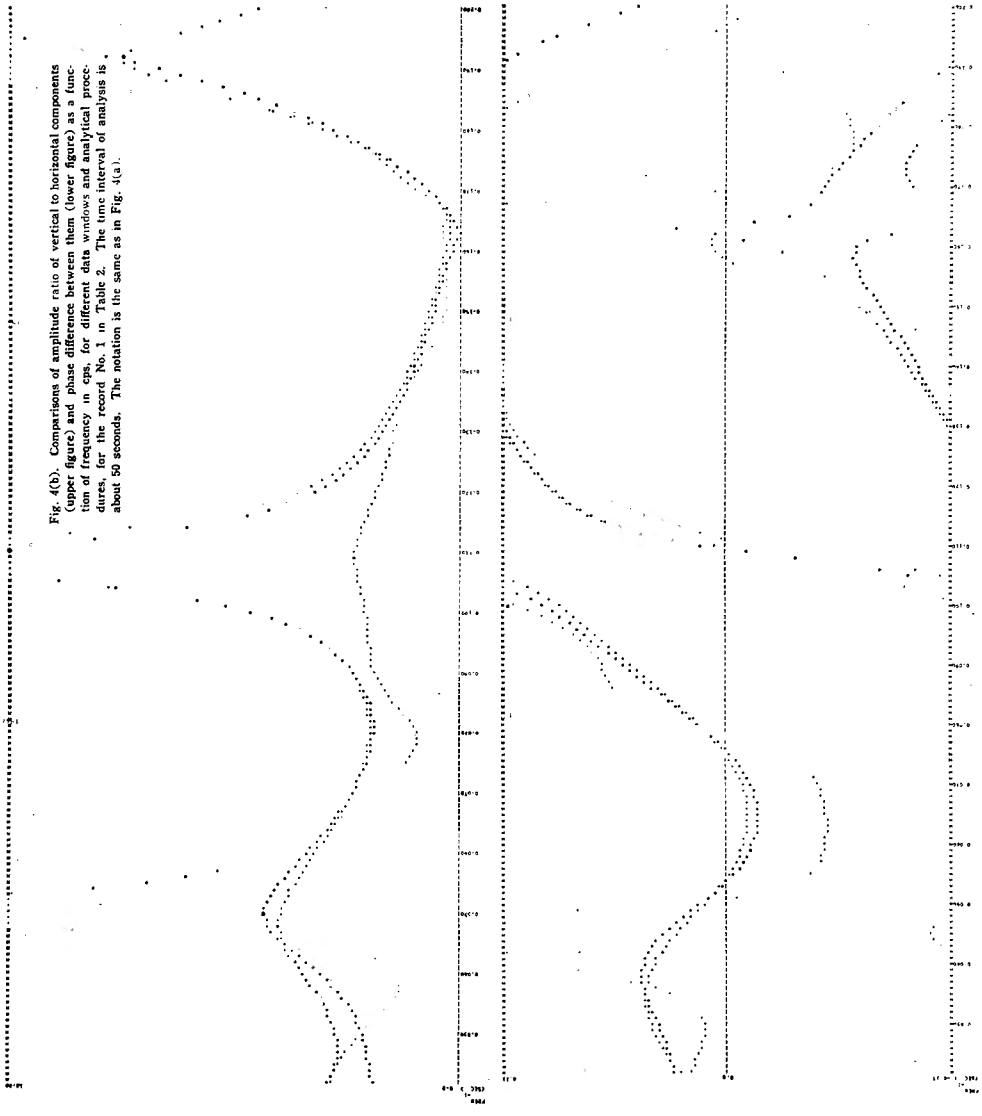

Fig. 4(b). Comparisons of amplitude ratio of vertical to horizontal components (upper figure) and phase difference between them (lower figure) as a function of frequency in cps, for different data windows and analytical procedures, for the record No. 1 in Table 2. The time interval of analysis is about 50 seconds. The notation is the same as in Fig. 4(a).

for different time intervals of analysis.

Theoretically it is difficult to discuss rigorously the difference between $\left\{\frac{1}{2\pi}F(\omega)*W(\omega)\right\}\Big/F_s(\omega)$ in (7) and $\left\{\frac{1}{2\pi}F(\omega)/F_s(\omega)\right\}*W(\omega)$ in (8). Also from the observational side, it is generally difficult, since numerical errors are not necessarily small in the step (B) of (8). Here a comparison has been made of the resultant $\bar{F}(\omega)$'s obtained by the two, steps (A) and (B) in (7) and those (A), (B), (C) and (D) in (8), for the record No. 1 in Table 2, taking the Fejér kernel window $w_5(t)$ as a data window. In the step (B) in (8), frequencies from 0.022 to 0.200 cps are taken at an interval of 0.002 cps. When the time interval is as long as over 100 seconds, the difference in $\bar{F}(\omega)$ between the two becomes appreciable for frequencies over about 0.15 cps, as shown in Figs. 3(a) and 4(a). (All the phase spectra in this paper are shown in parts of circle.) On the other hand, when the time interval of analysis is as short as 50 seconds, the difference is noticeable also for frequencies below about 0.05 cps, as shown in Figs. 3(b) and 4(b). For the power window $w_2(t)$, the difference is found to be small, even when a time interval of analysis is as short as 50 seconds.

From the insufficient examples above, we do not conclude the difference quantitatively in detail, but the above facts, especially relating to the uncertainty of peak positions for "heavy" data windows, should be borne in mind in the analysis of seismograms.

4. Effects of later phases on the spectra of initial phase

Generally the observed waveform $f(t)$ is considered to be composed of the sum of transient time functions $g_i(t)$ with random time lags of t_i seconds from the beginning of a primary arrival. With $F(\omega)$ and $G_i(\omega)$, the Fourier transforms of $f(t)$ and $g_i(t)$, respectively, we have

$$\left.\begin{aligned} f(t)&=\sum_{i=0}^{\infty}g_i(t-t_i),\\ F(\omega)&=\sum_{i=0}^{\infty}G_i(\omega)\exp(-i\omega t_i). \end{aligned}\right\} \tag{9}$$

Taking t_0 as zero and substituting $G(\omega)$ for $G_0(\omega)$, we have

$$F(\omega)=G(\omega)\left\{1+\sum_{i=1}^{\infty}G_i(\omega)/G(\omega)\quad\exp(-i\omega t_i)\right\}.$$

When later arrivals are of modulate forms of the primary arrival, we have

$$G_i(\omega)=T_i(\omega)G(\omega),$$

where we name $T_i(\omega)$ the modulation function.

Now we assume that $T_i(\omega)$ is independent of frequency, namely $T_i(\omega)=a_i$, which is approximately valid, for example, for the incidence of a pP phase

whose path is not substantially different from that of an initial P phase. An example is shown in Figs. 5(a) and (b), with the observed waveforms, when a strong pP phase is incident at about 50 seconds after the incidence of an initial P phase. It appears that the amplitude and phase spectra of P and pP phases are similar to each other. As shown in Figs. 5(c) and (d), similarity is more apparent in the spectra of the amplitude ratio and phase difference except for the frequency range lower than about 0.020 cps where their reliability is low.

Thus it follows

$$\left.\begin{aligned} f(t) &= \sum_{i=0}^{\infty} a_i g(t-t_i), \\ F(\omega) &= G(\omega) \sum_{i=0}^{\infty} a_i \exp(-i\omega t_i), \end{aligned}\right\} \tag{10}$$

where a_0 is taken as 1. Without loss of generality, a_i may be assumed as being quite small except for the first few arrivals. The positiveness and negativeness of a_i $(i \geq 1)$ mean the identity and opposition of the incident direction of later phases to that of the initial phase, respectively. The amplitude and phase spectra of the second factor in the righthand side of the above expression are

$$\left.\begin{aligned} A(\omega) &= \left\{ \sum_{i=0}^{\infty} a_i^2 + 2 \sum_{\substack{i=0 \\ i>j}}^{\infty} a_i a_j \cos \omega (t_j - t_i) \right\}^{1/2}, \\ P(\omega) &= \tan^{-1}\left(- \sum_{i=0}^{\infty} a_i \sin \omega t_i \Big/ \sum_{i=0}^{\infty} a_i \cos \omega t_i \right). \end{aligned}\right\} \tag{11}$$

Thus, when later phases are incident, the amplitude spectrum of the initial phase is multiplied by $A(\omega)$ and its phase spectrum advances by $P(\omega)$. Therefore, if the amplitude and phase spectra of an initial phase are rather smooth, troughs of the amplitude spectrum and steep advances of the phase spectrum are introduced by the incidence of later phases, as will be seen below.

(1) Now we consider the case when only a later phase follows the initial phase. This has already been examined by Kishimoto [1964]. In this case, the expressions (10) and (11) reduce to

$$\left.\begin{aligned} f(t) &= g(t) + a_1 g(t-t_1), \\ F(\omega) &= G(\omega)\{1 + a_1 \exp(-i\omega t_1)\}, \end{aligned}\right\}$$

and

$$\left.\begin{aligned} A(\omega) &= (1 + a_1^2 + 2a_1 \cos \omega t_1)^{1/2}, \\ P(\omega) &= \tan^{-1}\{-a_1 \sin \omega t_1 / (1 + a_1 \cos \omega t_1)\}. \end{aligned}\right\} \tag{12}$$

These functions are plotted in Fig. 6, in which t_1 and a_1 are taken as 50 seconds, and -0.5, -1.0, 0.5, 1.0 and 1.5. For a_1 other than these values, the corresponding spectra can be interpolated or extrapolated. These spectra gener-

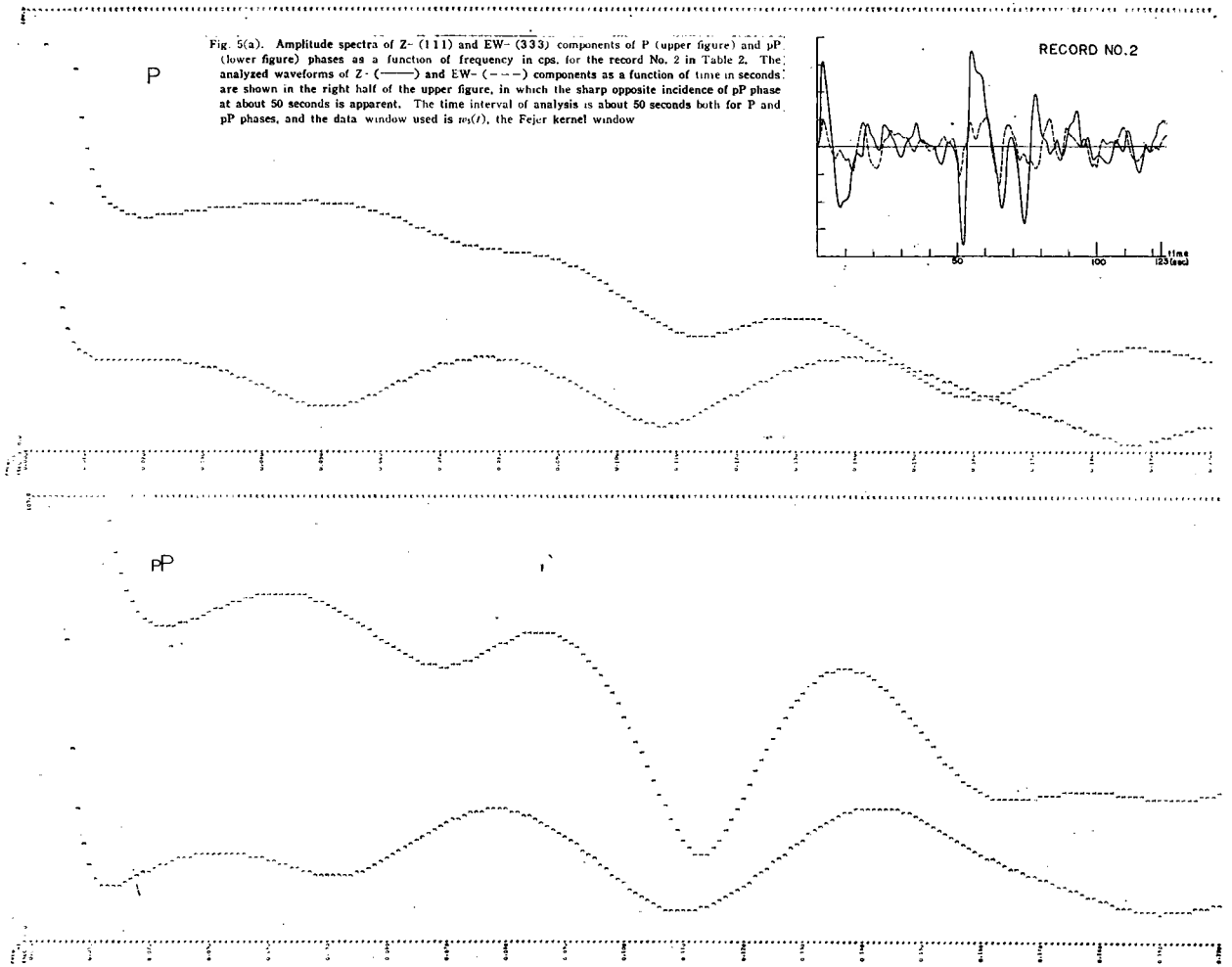

Fig. 5(a). Amplitude spectra of Z- (111) and EW- (333) components of P (upper figure) and pP (lower figure) phases as a function of frequency in cps. for the record No. 2 in Table 2. The analyzed waveforms of Z- (——) and EW- (– – –) components as a function of time in seconds are shown in the right half of the upper figure, in which the sharp opposite incidence of pP phase at about 50 seconds is apparent. The time interval of analysis is about 50 seconds both for P and pP phases, and the data window used is $w_3(t)$, the Fejer kernel window

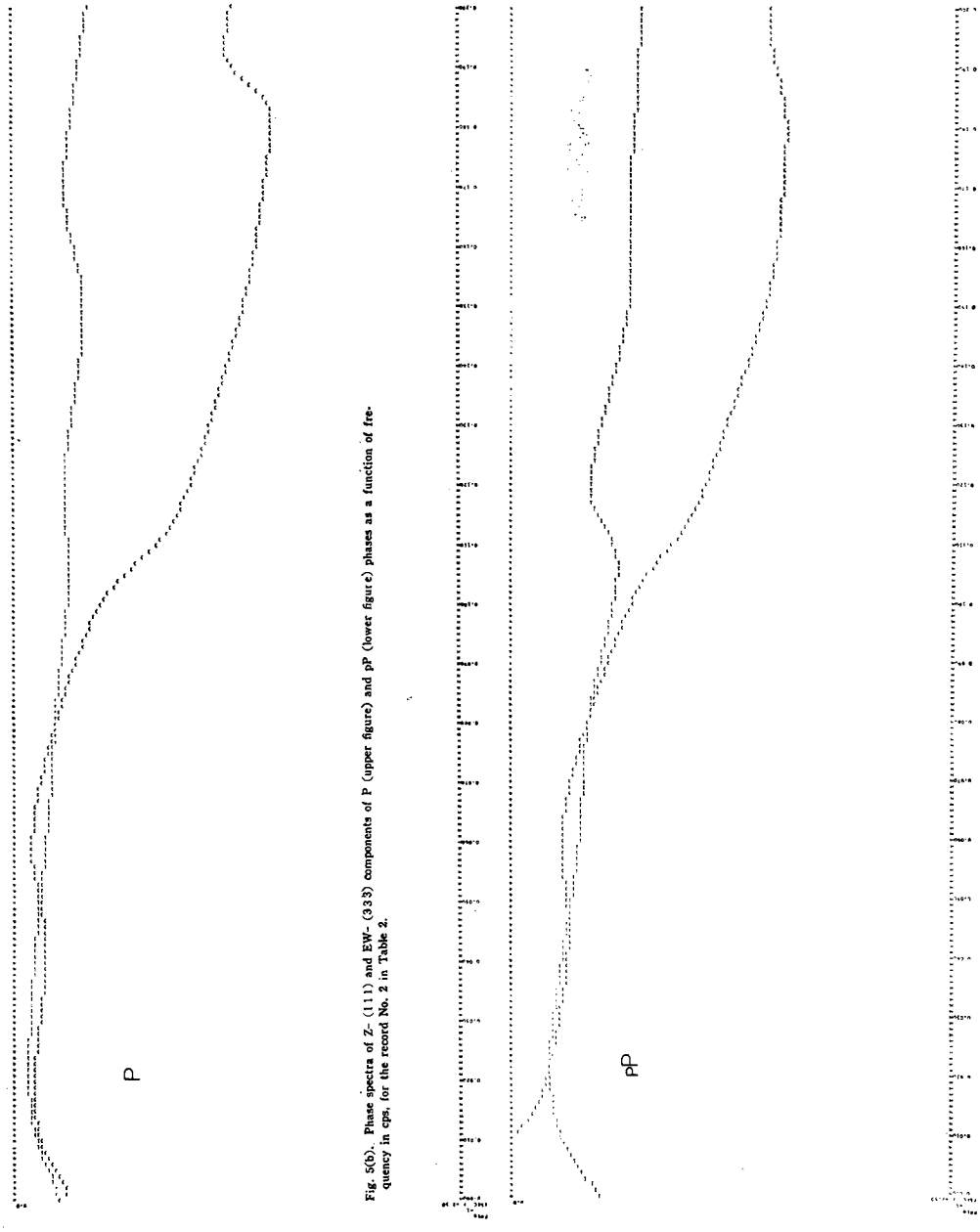

Fig. 5(b). Phase spectra of Z- (111) and EW- (333) components of P (upper figure) and pP (lower figure) phases as a function of frequency in cps, for the record No. 2 in Table 2.

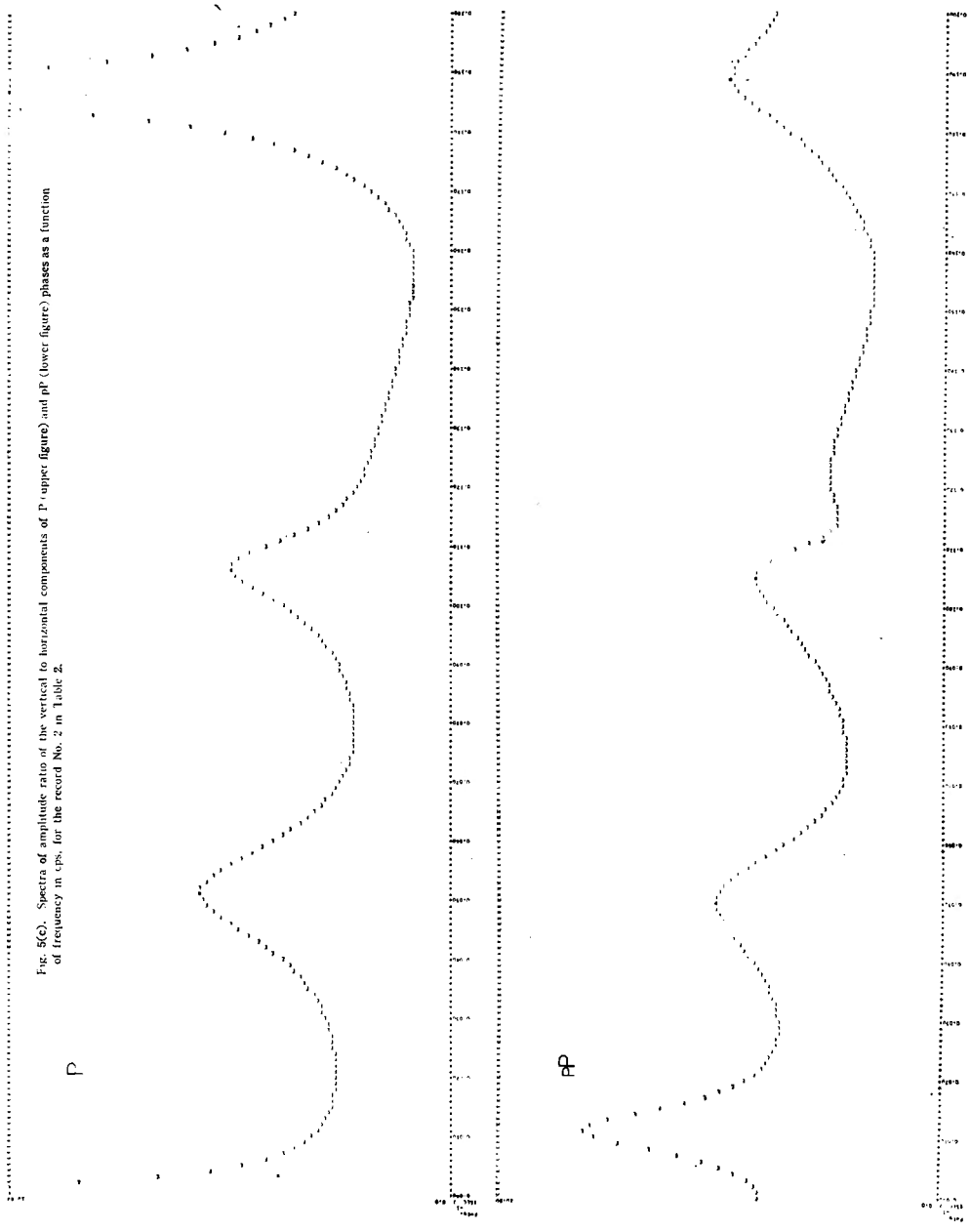

FIG. 5(c). Spectra of amplitude ratio of the vertical to horizontal components of P (upper figure) and pP (lower figure) phases as a function of frequency in cps, for the record No. 2 in Table 2.

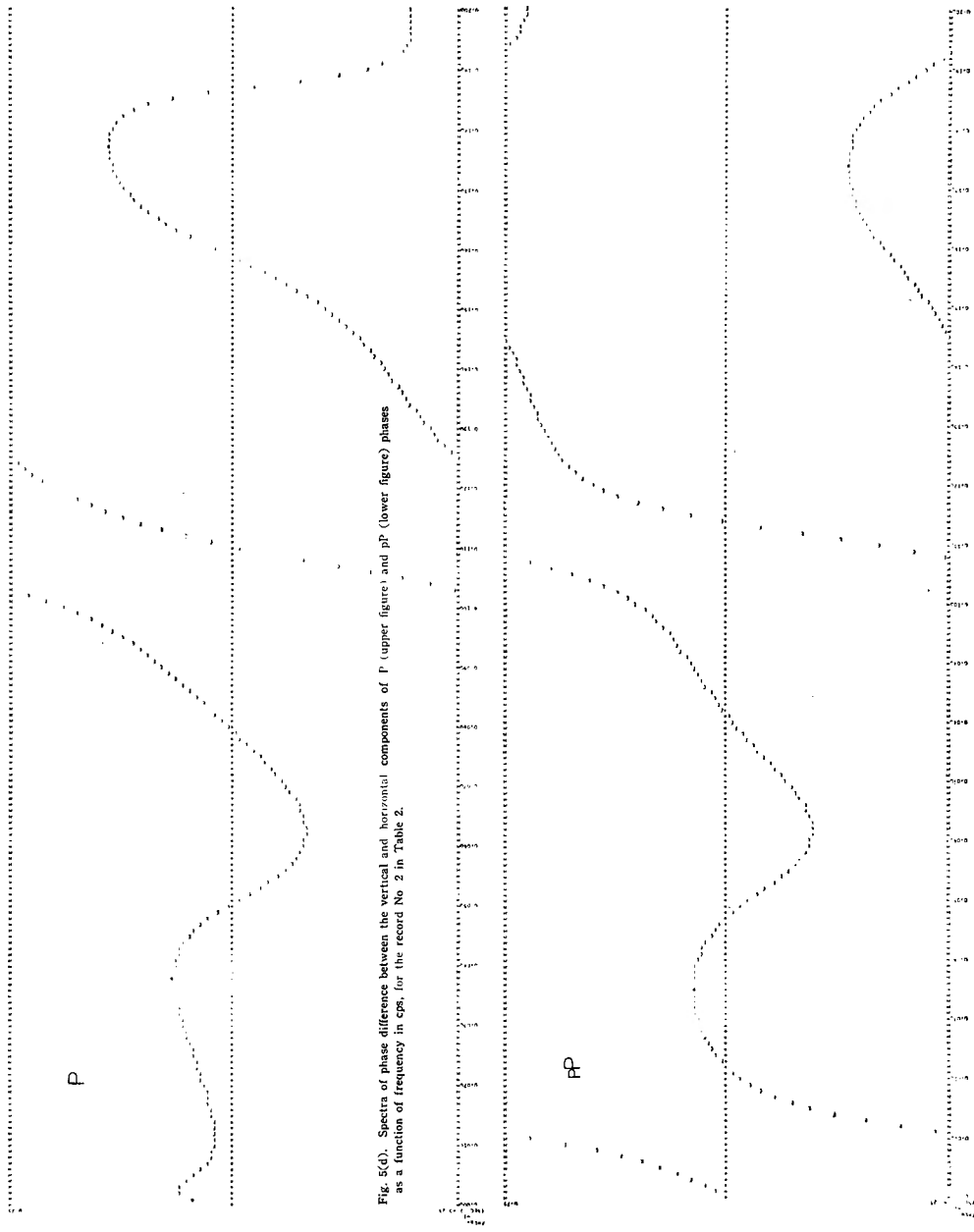

Fig. 5(d). Spectra of phase difference between the vertical and horizontal components of P (upper figure) and pP (lower figure) phases as a function of frequency in cps, for the record No 2 in Table 2.

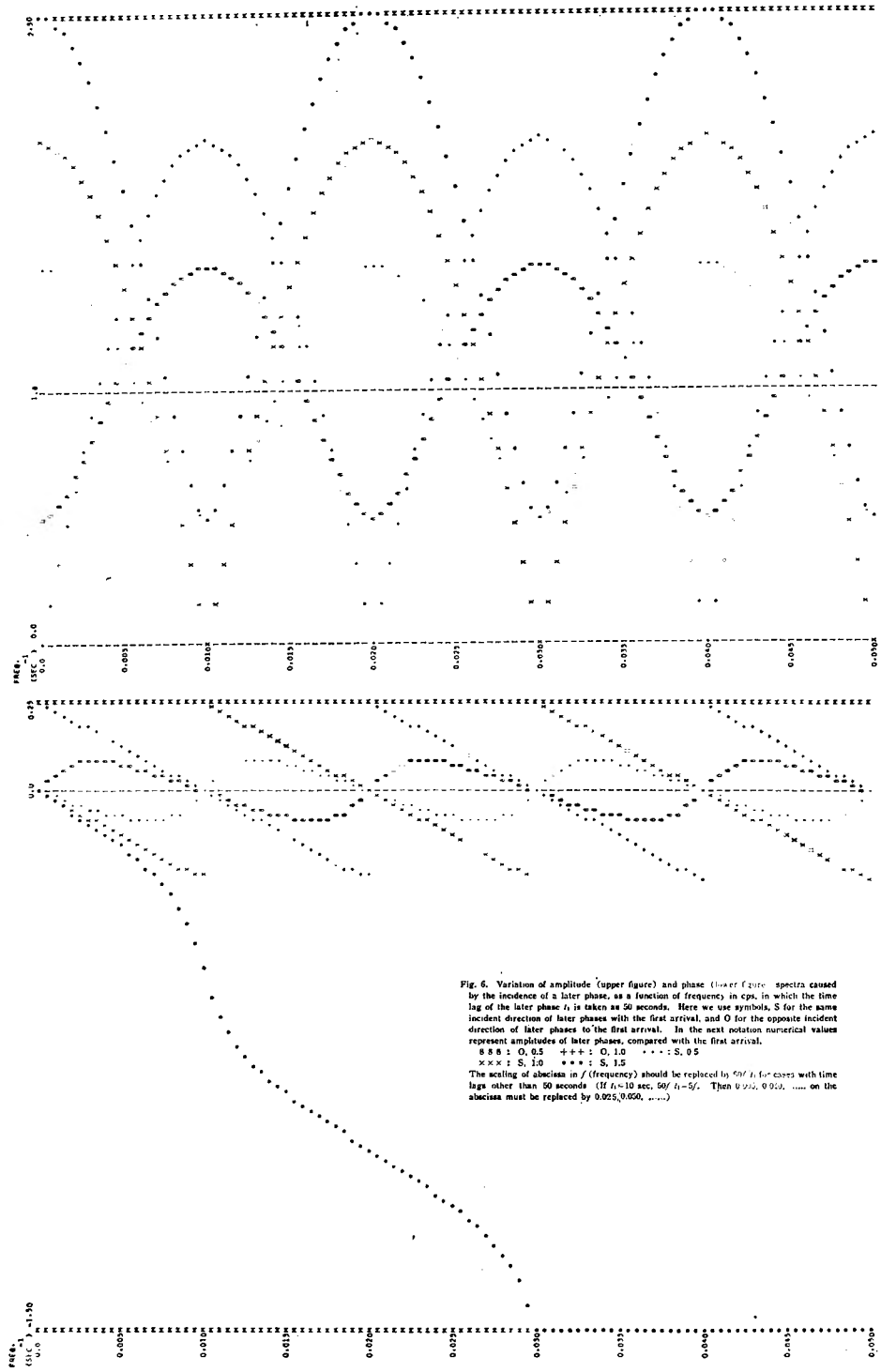

Fig. 6. Variation of amplitude (upper figure) and phase (lower figure) spectra caused by the incidence of a later phase, as a function of frequency in cps, in which the time lag of the later phase t_1 is taken as 50 seconds. Here we use symbols, S for the same incident direction of later phases with the first arrival, and O for the opposite incident direction of later phases to the first arrival. In the next notation numerical values represent amplitudes of later phases, compared with the first arrival.

8 8 8 : O, 0.5 +++ : O, 1.0 • • • : S, 0.5
× × × : S, 1.0 • • • : S, 1.5

The scaling of abscissa in f (frequency) should be replaced by $50/t_1$ for cases with time lags other than 50 seconds (If t_1=10 sec, $50/t_1=5$. Then 0.025, 0.050, ... on the abscissa must be replaced by 0.025,0.050, ...)

ally show a sinusoidal oscillation, the period of which is $\omega t_1=2\pi$ or $f=0.02$ cps. From expression (12), it readily follows that for the amplitude spectrum minima occur at $\omega t_1=(2n+1)\pi$ or $f=\frac{2n+1}{2t_1}$ when $a_1>0$, and at $\omega t_1=2n\pi$ or $f=\frac{n}{t_1}$ when $a_1<0$ ($n=0, 1, 2, \ldots\ldots$), and for the phase spectrum its characteristics can be tabulated by the following, in which when $|a_1|>1$ the phase spectrum decreases monotonically, 2π for $\omega t_1=2\pi$ or $f=\frac{1}{t_1}$.

	$a_1>1$	$a_1=1$	$\lvert a_1\rvert<1$	$a_1=-1$	$a_1<-1$
at $\omega t_1=2n\pi$ or $f=\frac{n}{t_1}$		zero	zero	jump by π	steep decrease
at $\omega t_1=(2n+1)\pi$ or $f=\frac{2n+1}{2t_1}$	steep decrease	jump by π	zero	zero	

Fig. 7(a) shows the amplitude and phase spectra of a record with a time interval of analysis of about 123 seconds in which the initial P phase is followed by a pP phase with the opposite incidence at about 50 seconds. Characteristics of these spectra are not affected by the lengthening or shortening of the time interval of analysis by 20 seconds or more, since there is no strong incidence of new phases in this time range. A comparison of Figs. 6 and 7(a) substantiates fairly well the above assumption, for troughs of the amplitude spectra and steep increase (or decrease) of phase spectra for the case when $a_1=-1.0$ in Fig. 6 occur at almost the same frequencies as the corresponding spectra in Fig. 7(a).

Fig. 7(b) shows the amplitude ratio of the vertical to horizontal components and the phase difference between them. It is noticed from the figure that these spectra distinctly conserve characteristics of amplitude and phase spectra respectively. This means that the effects of the incidence of later phases cannot be discharged by taking the amplitude ratio and phase difference only, though this effect seems to disappear in a simple mathematical consideration.

(2) Now we consider the case when two or more later phases follow the initial phase.

Figs. 8(a) and (b) show variations of the amplitude and phase spectra induced by the incidence of one to five later phases. The inciednce of two or more later phases distorts irregularily the spectra of the initial phase. For amplitude spectra, splitting of troughs occurs, and for phase spectra, a shift of peak positions occurs. For brevity, it is shown in this paper in the cases when later phases are incident with equal time lags, absolute amplitudes of which are one half of the immediately preceding phase. It is apparent from Figs. 6, 8 and others (not shown in this paper) that the incidence of many later phases with comparatively small amplitudes does not greatly affect the spectra of the

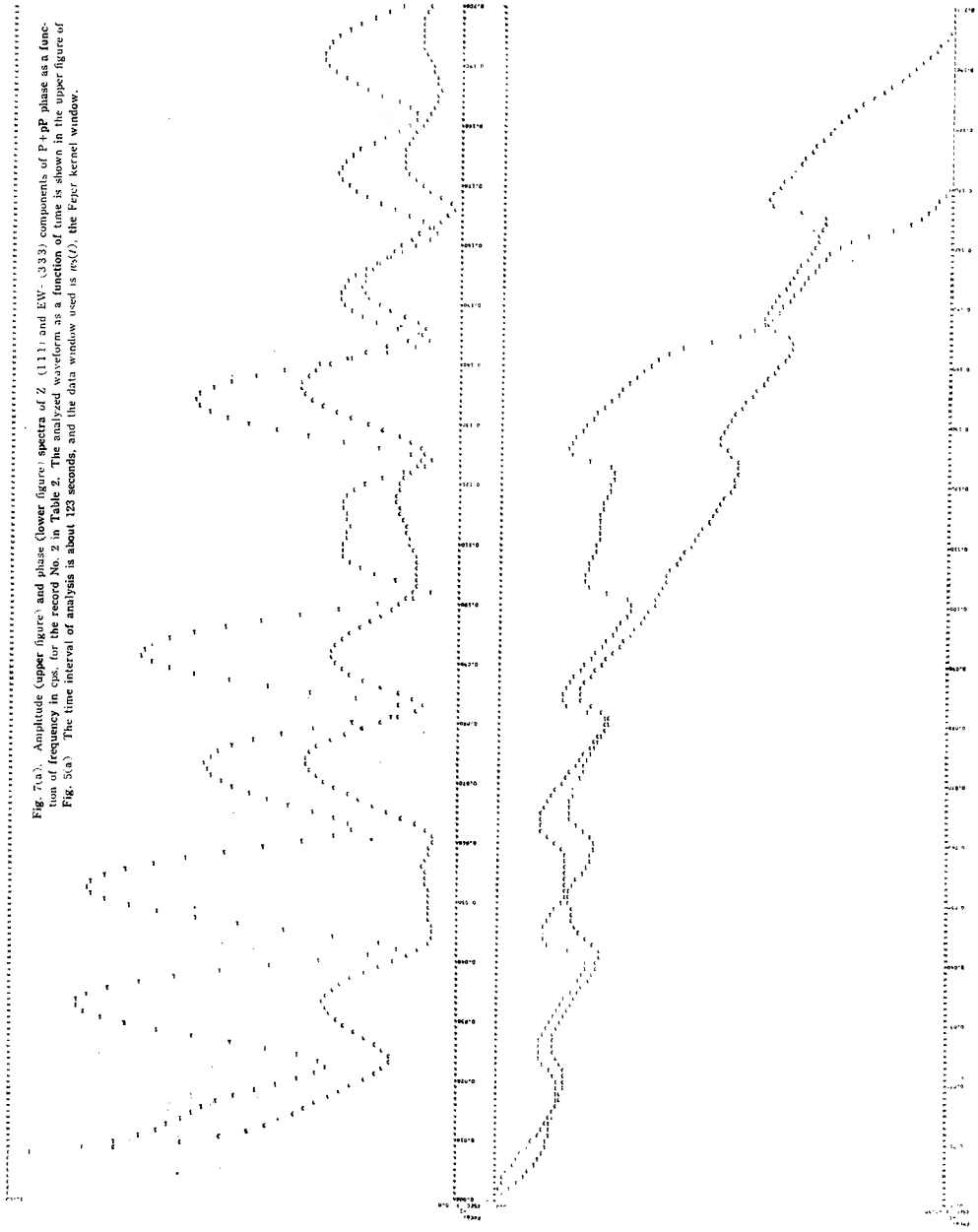

Fig. 7(a). Amplitude (upper figure) and phase (lower figure) spectra of Z (111) and EW (333) components of P+pP phase as a function of frequency in cps, for the record No. 2 in Table 2. The analyzed waveform as a function of time is shown in the upper figure of Fig. 5(a) The time interval of analysis is about 123 seconds, and the data window used is $w_3(t)$, the Fejer kernel window.

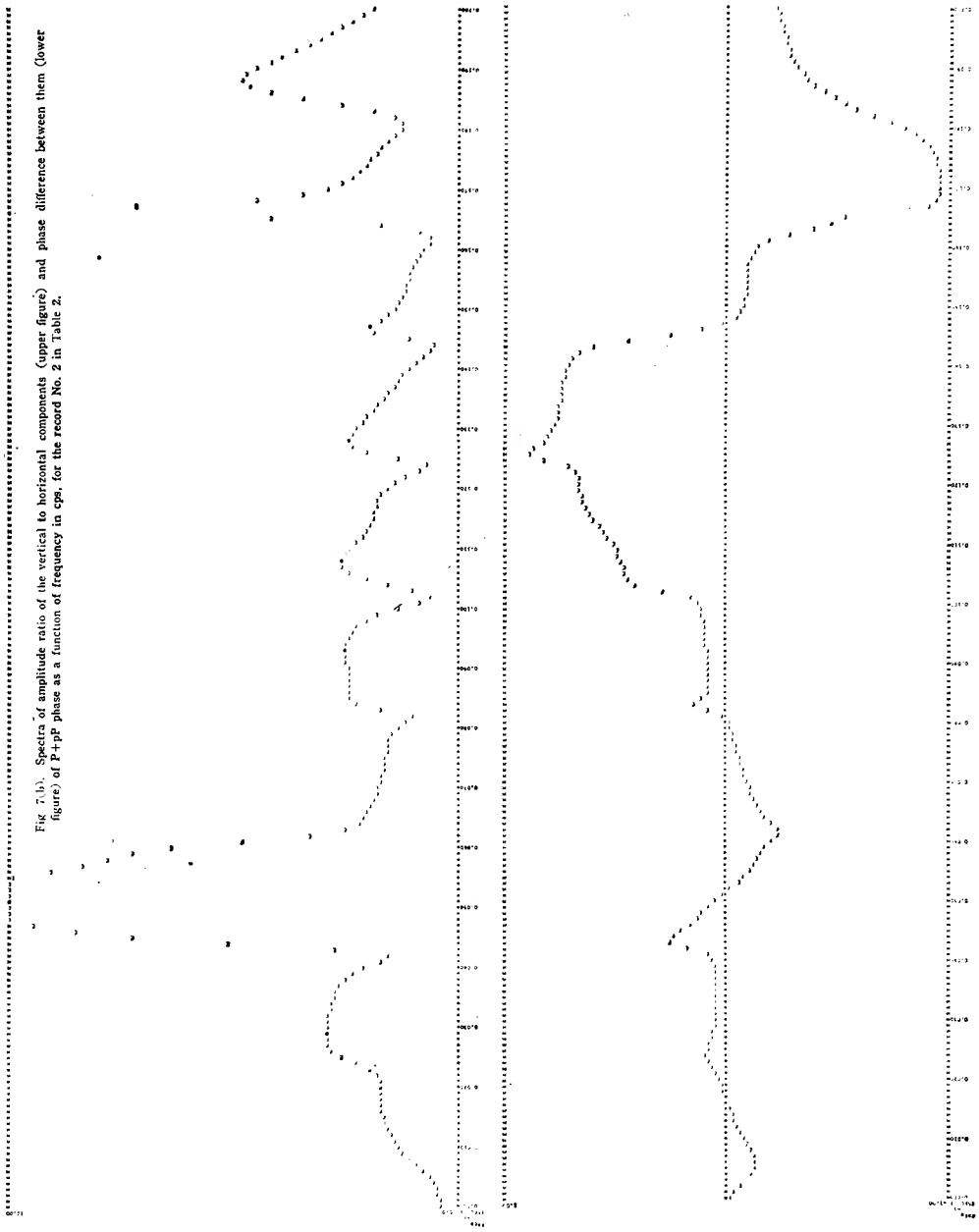

Fig. 7(b). Spectra of amplitude ratio of the vertical to horizontal components (upper figure) and phase difference between them (lower figure) of P+pP phase as a function of frequency in cps, for the record No. 2 in Table 2.

Fig. 8 a). Variation of amplitude (upper figure) and phase (lower figure) spectra caused by the incidence of some later phases, as a function of frequency in cps. The incident direction of later phases is the same as that of the initial phase, and t_1 is taken as 50 seconds and the absolute values of a_i's are as follows, except that a_i's ($i \neq 5$) are zero.

	$\lvert a_1 \rvert$	$\lvert a_2 \rvert$	$\lvert a_3 \rvert$	$\lvert a_4 \rvert$	$\lvert a_5 \rvert$
∗∗∗	$\lvert a_1 \rvert/2$	0	0	0	0
+++	$\lvert a_1 \rvert/2$	$\lvert a_2 \rvert/2$	0	0	0
···	$\lvert a_1 \rvert/2$	$\lvert a_2 \rvert/2$	$\lvert a_3 \rvert/2$	0	0
×××	$\lvert a_1 \rvert/2$	$\lvert a_2 \rvert/2$	$\lvert a_3 \rvert/2$	$\lvert a_4 \rvert/2$	0
∗·∗	$\lvert a_1 \rvert/2$	$\lvert a_2 \rvert/2$	$\lvert a_3 \rvert/2$	$\lvert a_4 \rvert/2$	$\lvert a_5 \rvert/2$

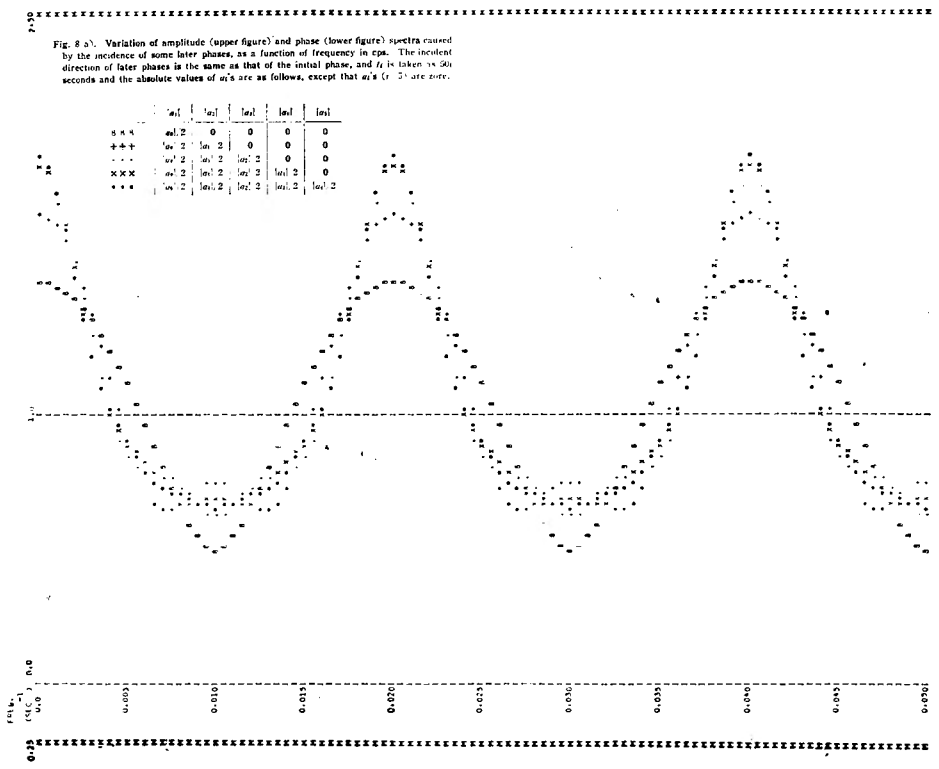

Fig. 8 b). Variation of amplitude (upper figure) and phase (lower figure) spectra caused by the incidence of some later phases as a function of frequency in cps. The incident direction of later phases is the opposite of that of the initial phase. The absolute values of a_i's are the same as in Fig. 8(a).

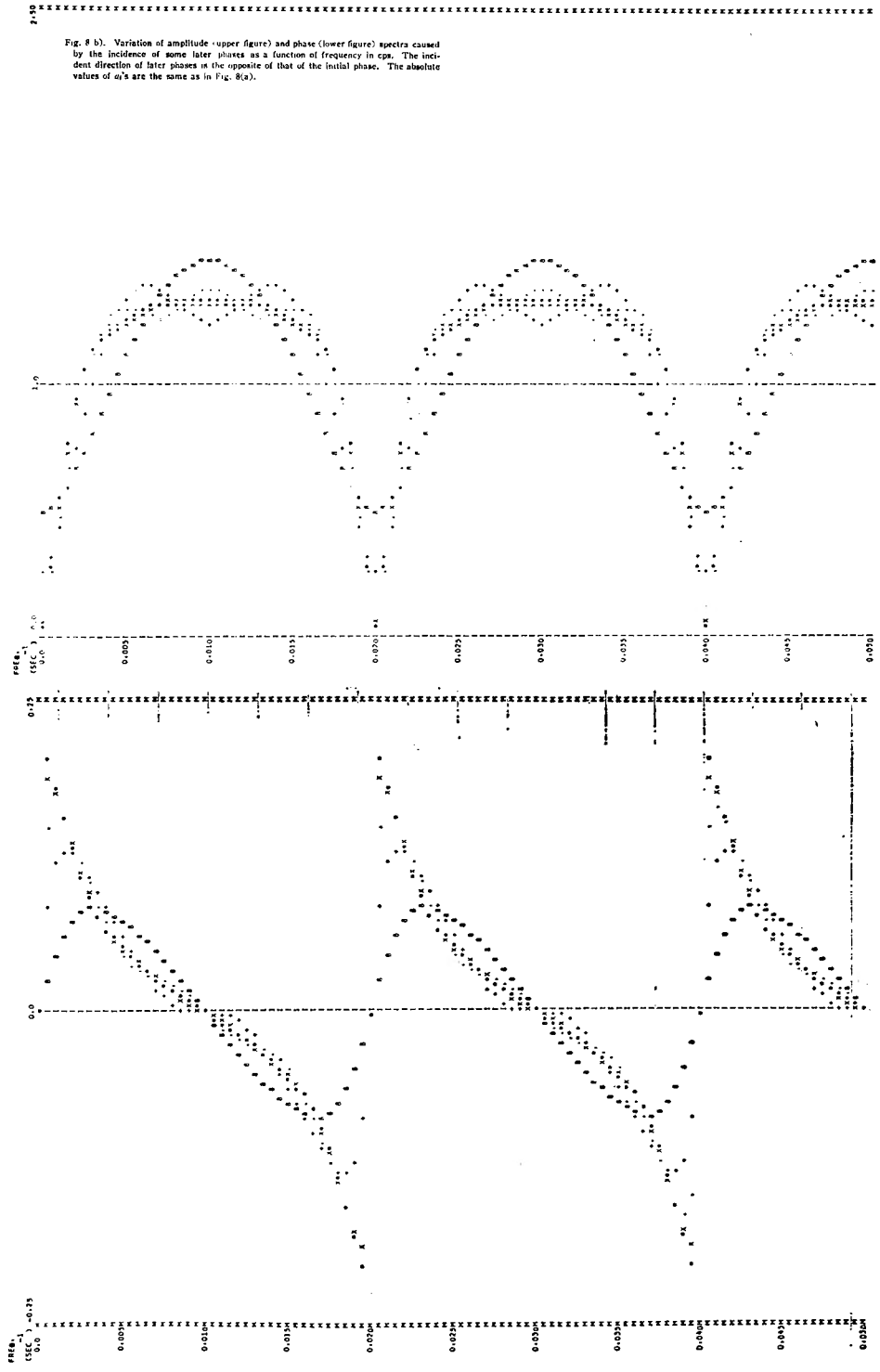

initial phase.

For the incidence of later phases of near-source reflections in the case of shallow shocks, a precise incident time is generally difficult to discern on seismograms, which causes the uncertainty of trough positions. In this case, however, spacing of troughs is widespread and the spectra vary rather smoothly with frequency.

From the above considerations, it follows that if we wish to discuss fine spectral structure of the initial phase when the time interval of analysis contains later phases with large amplitude, the next procedure is to be followed. If time lags of the later phases are large, the time interval of analysis should be truncated before those incidences. If time lags of the later phases are small, the time interval of analysis should contain these incidences and in the frequency domain resultant illusive troughs should be omitted, which may appear with regular spacing.

Acknowledgements

It is a pleasure to thank Dr. Takeshi Mikumo for his critical review of this manuscript. This study was begun when the author was a graduate student at the Geophysical Institute, Faculty of Science, Kyoto University. The data have been obtained from the Matsushiro Seismological Observatory, one of the USCGS World-wide Standardized Network Stations. The computation was carried out on a FACOM 230-60 at Kyoto University Data Processing Center and on a HITAC 5020 at Kyoto University Computation Center.

References

Fernandez, L. M. and J. Careaga, 1968; The thickness of the crust in central United States and La Pas, Bolivia, from the spectrum of longitudinal seismic waves, Bull. Seism. Soc. Amer., 58, 711–741.

Holloway, J. L., Jr., 1958; Smoothing and filtering of time series and space fields, *Advances in Geophysics*, 4, 351–389.

Kishimoto, Y., 1964; Investigation on the origin mechanism of earthquakes by the Fourier analysis of seismic body waves (1), Bull. Dis. Prev. Inst., Kyoto Univ., **67**, 18–37.

Kurita, T., 1966; Attenuation of long-period P-waves and Q in the mantle, J. Phys. Earth, 14, 1–14.

Kurita, T., 1969; Crustal and upper mantle structure in Japan from amplitude and phase spectra of long-period P-waves, Part 1. Central mountain area, J. Phys. Earth, **17**, 13–41. Part 2. Kanto plain, Special Contributions, Geophys. Inst., Kyoto Univ., No. **9**, 137–166.

Papoulis, A., 1962; *The Fourier integral and its applications*, MaGraw-Hill, New York. 318 pp.

Wood, L. C., 1968; A review of digital pass filtering, Rev. Geophys., 6, 73–97.